ELSEVIER

Journal of Magnetism and Magnetic Materials 164 (1996) 357–366

journal of magnetism and magnetic materials

Heat treatment effects on structural and magnetic properties of fine Fe–B particles

L. Yiping [a], G.C. Hadjipanayis [b,*], V. Papaefthymiou [c], A. Kostikas [d], A. Simopoulos [d], C.M. Sorensen [e], K.J. Klabunde [f]

[a] *Institute for Energy Conversion, University of Delaware, Newark, DE 19716, USA*
[b] *Department of Physics and Astronomy, University of Delaware, Newark, DE 19716-2570, USA*
[c] *Department of Physics, University of Ioannina, Ioannina, Greece*
[d] *National Center for Scientific Research 'Demokritos,' Athens, Greece*
[e] *Department of Physics, Kansas State University, Manhattan, KS 66506, USA*
[f] *Department of Chemistry, Kansas State University, Manhattan, KS 66506, USA*

Received 1 May 1996; revised 8 May 1996

Abstract

The structural and magnetic properties of fine Fe–B particles with a size of about 50 nm and B concentrations of 5, 14, and 17 at.% were studied in as-prepared samples and after annealing in vacuum and in H_2 atmosphere. The samples annealed in vacuum were found to be dominated by α-Fe in the high B concentrations. Oxide components appear in the particles with low B content. Boron is found to prevent oxidation of the as-made samples and promote the formation of mixed valence oxides in the crystallized samples.

Keywords: Mössbauer spectroscopy; Fine particles; Particles – fine

1. Introduction

Since the initial report of Schlesinger et al. [1] that transition metal boron powders can be produced by chemical reduction with $NaBH_4$, a number of studies have been focused on the sample preparation, crystallization behavior, and structural and magnetic properties of Fe–B, Co–B, Fe–Co–B, and Fe–Ni–B particles produced by this technique [2–6]. In the borohydride reduction of hydrolyzed metal salts, the metallic cations are reduced to metal atoms which subsequently nucleate and agglomerate to form larger particles. From the results of our previous studies on Fe–B, Fe–Co–B, and Co–B systems [7–11], as well as those of other investigators [12], it is known that the preparation conditions including the solution concentration and pH, the mixing procedure, and the atmosphere under which sample preparation is performed influence strongly the chemical composition, the particle size, the particle morphology and the crystal structure and consequently the magnetic properties of the products. Further modification of the magnetic and structural properties is obtained by heat treatment. It is therefore of considerable interest

* Corresponding author. Fax: +1-302-831-1637.

PII S0304-8853(96)00405-2

both for fundamental reasons and for potential applications to elucidate the role of the preparation parameters and to establish the conditions for synthesis of stable particles with optimized properties.

Our previous studies of Co–B and Fe–Co–B systems [8,9] have shown that, to a first approximation, higher concentration solutions produce smaller particles, because at higher concentrations the reduction is faster and more nuclei are formed, so that fewer metal atoms are available to promote particle growth. In Co–B and Fe–Co–B systems the particle size could be varied by this method from 40 to 90 nm and 15 to 55 nm, respectively. On the other hand, the composition and structure of the particles is strongly affected by the mixing procedure. The maximum amount of boron in Fe–B particles was 15% when the 'Y junction' technique was used; reduction by adding (drop by drop) the alkaliboride to the metal salt solution with vigorous stirring leads to particles with higher boron content and with an amorphous structure [7]. Linderoth et al. [12] reported that amorphous $Fe_{62}B_{38}$ particles were obtained by reduction of $FeSO_4$ with KBH_4 using the 'dropwise' method. Crystalline Fe_2B and α-Fe were found to form when the particles were annealed in Ar and H_2 with the ratio of α-Fe to Fe_2B depending on the annealing time and temperature. In Co–B particles the behavior appears to be different and amorphous powders with high boron content (up to 40%) can be produced even with the 'Y junction' technique. For example, in a recent study of the Co–B system, we have found that amorphous Co_2B particles can be obtained by rapidly mixing the two solutions under anaerobic conditions [12]. The enhancement of B concentration by the presence of Co has also been observed by Wells et al. [13].

While the studies to date have provided considerable information on the structure and composition of Fe–B, Co–B, and Fe–Co–B particles, there exist relatively fewer results on the magnetic properties. More specifically, the dependence of magnetization and coercivity, which are technologically important parameters, on the boron content, particle size, and heat treatment has not been studied in detail. Our previous studies have indicated that coercive fields of up to 2 kOe can be achieved in the Fe–Co–B system [9].

In the present study we have investigated the dependence of the magnetic properties of Fe–B particles on boron content in as-prepared as well as heat treated samples. The variation in B content was achieved by keeping the concentration of the reacting solutions constant and varying only the rate of addition of the alkaline borohydride solution into the ferric chloride solution. From previous results, this procedure is expected to lead to Fe–B particles of approximately constant size but with different B content.

2. Experimental methods

The Fe–B particles in the present study were prepared by adding the alkaline borohydride solution 'dropwise' into the ferric chloride solution in air while stirring vigorously. The precipitants were washed with distilled water and acetone and dried in a flow of Ar gas. Fine Fe–B particles with a constant size but different B content were obtained by varying the rate of adding $NaBH_4$ into $FeCl_3$ while keeping the concentration of the $FeCl_3$ and $NaBH_4$ solutions constant at 0.08 and 0.025 M, respectively. Using flow rates for the $NaBH_4$ addition of 1, 20, and 70 ml/min, Fe–B particles were obtained with compositions $Fe_{95}B_5$, $Fe_{86}B_{14}$, and $Fe_{83}B_{17}$, respectively, as determined by inductively coupled plasma (ICP) emission spectroscopy.

Heat treatments were carried out in vacuum and in a gas flow of H_2. For vacuum annealing, the samples were sealed in a quartz tube under a pressure of $\sim 10^{-5}$ mbar and heated to temperatures between 400 and 600°C for various times. Annealings under H_2 atmosphere were done in the same temperature range by heating the samples in a quartz tube, in flowing H_2 gas. After the heat treatment the powders were cooled to room temperature in an Ar atmosphere. The processed powders were passivated in a similar way as the as-prepared samples, apparently because of oxygen admixtures in the Ar gas.

The size and morphology of the particles were determined by transmission electron microscopy (TEM) using a JEOL-100C electron microscope. X-ray diffraction powder patterns were used to determine the structure (amorphous or crystalline) and phase constitution of the samples. A SQUID magnetometer and a vibrating sample magnetometer were

used to measure the magnetic properties (magnetization and coercive field) in the temperature range of 10–870 K. Mössbauer spectra were obtained with a conventional constant acceleration spectrometer with a ^{57}Co(Rh) source in the temperature range 4.2–300 K. Differential scanning calorimetry (DSC) was used to determine the crystallization temperature of the amorphous samples in the temperature range of 100 to 600°C with a heating rate of 10°C/min.

3. Results

3.1. Structure, morphology, and phase constitution

Microstructure studies showed that the particles have a nearly spherical shape with a fairly uniform size of ~ 50 nm for all samples. A tendency of the particles to form chains was also observed. Typical transmission electron micrographs of two of the as-made samples with boron content 5 and 17% are shown in Fig. 1a,b, respectively.

The X-ray diffraction patterns of the three as-made samples with boron content 5% (a), 14% (b), and 17% (c) are shown in Fig. 2A. The high-B-content sample shows a typical amorphous-like structure.

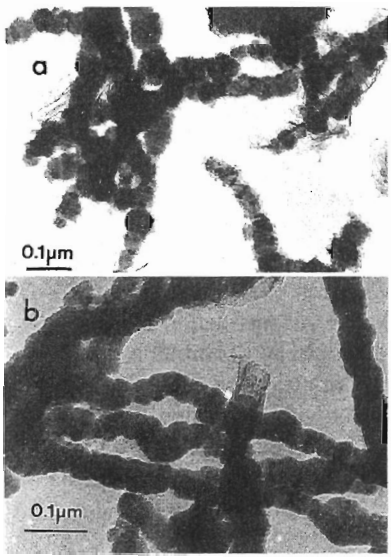

Fig. 1. Electron micrographs of Fe–B particles (a) with 5% B content and (b) with 17% B content.

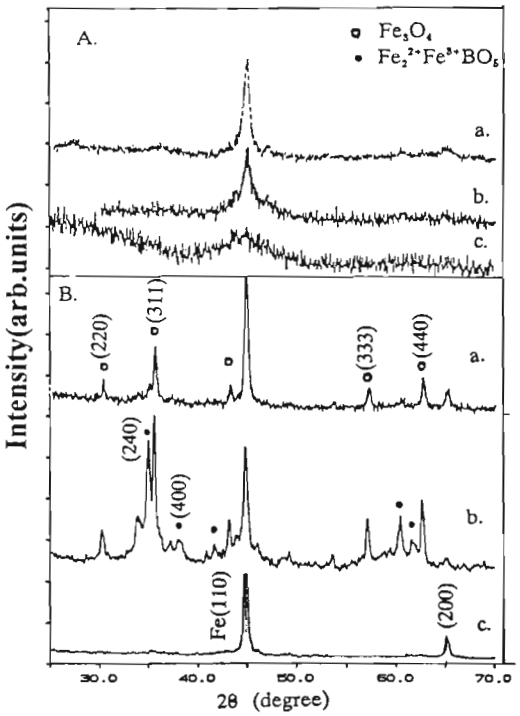

Fig. 2. X-ray diffraction patterns of as-made and annealed samples of Fe–B particles. (A) As-made particles with (a) 5%, (b) 14%, and (c) 17% B content. (B) Particles annealed at 500°C in vacuum for 1 h with (a) 5%, (b) 14%, and (c) 17% B content.

With decreasing B content sharper peaks corresponding to α-Fe appear superimposed on the broad peaks of the amorphous component, indicating that the particles consist of a mixture of amorphous and microcrystalline phases.

DSC measurements of the as-made samples are shown in Fig. 3. The high-B-content sample (Fig. 3c) shows a sharp exothermic peak at 475°C upon heating, indicative of crystallization of the amorphous phase. The low (5%) B-content sample shows no crystallization peaks (Fig. 3a). The intermediate (14%) B-content sample shows more complicated behavior indicating several phase transformations (Fig. 3b). The nature of the phases present is clarified by the results on the annealed samples which are discussed in the following section.

The effect of annealing the samples at 500°C for 1 h in vacuum is shown in the X-ray diffraction patterns of Fig. 2B. The low-boron-content particles

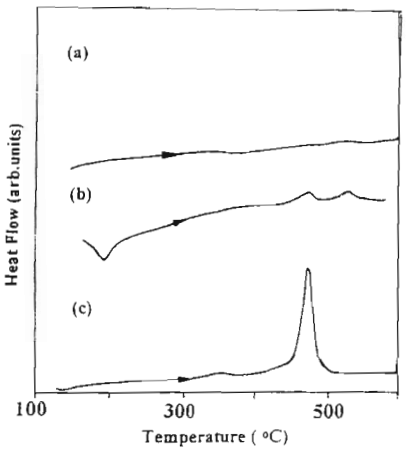

Fig. 3. Differential scanning calorimetry measurements of Fe–B particles with B content of (a) 5%, (b) 14%, and (c) 17%.

show α-Fe and Fe_3O_4 phases with α-Fe as the majority phase. In the medium-B-content sample an additional phase appears which could be indexed as the mixed valence iron borate $Fe_2^{2+}Fe^{3+}BO_5$ [14]. A single α-Fe phase is observed in the high-B-content powders. Annealing at 600°C for 1 h leads to X-ray patterns which show a majority α-Fe and minority Fe–O and $Fe_2^{2+}Fe^{3+}BO_5$ phases for the 5% B sample, $Fe_2^{2+}Fe^{3+}BO_5$ phase in the 14% B sample, and sharp α-Fe peaks in the 17% B sample. In the latter sample, longer annealing (24 h) at 600°C leads to the appearance of Fe_2B. Similar results for high boron content particles have been obtained by Linderoth et al. [12].

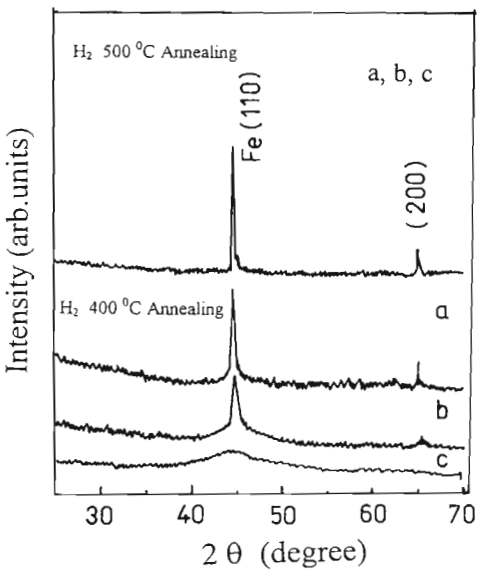

Fig. 4. XRD patterns of Fe–B particles annealed in H_2 at 400 and 500°C for 1 h.

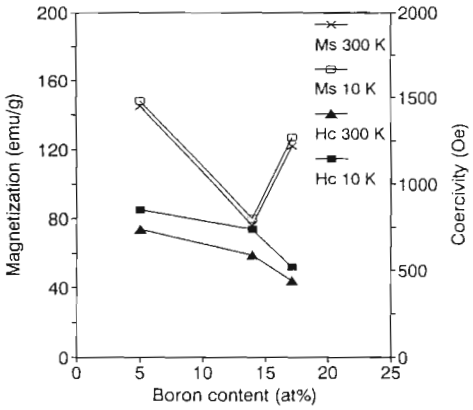

Fig. 5. Saturation magnetization M_s and coercive field H_c versus B content for as-made FeB particles at 10 and 300 K.

Annealing of the powders in H_2 atmosphere yields different results. Heating at 500°C for 1 h results in an X-ray pattern which shows essentially only α-Fe for all three B compositions (Fig. 4). Annealing at 400°C for 1 h produces no significant change in the X-ray patterns in comparison to the diffractograms of the as-made samples. Significant changes, however, occur in the magnetic properties as will be shown below.

3.2. Magnetic properties

The saturation magnetization M_s of the as-made particles as a function of B content is shown in Fig. 5 for two temperatures (10 and 300 K). In the same figure the values of the coercive field H_c are also presented. The magnetization is highest for the low-B-content sample and exhibits a dip in the medium-B-content sample. The coercive field decreases monotonously with increasing B content. The dependence of magnetization on B content is consistent with our previous results [7] and can be attributed to Fe–B and Fe–O phases, as discussed in the next section.

The changes in magnetization upon annealing are illustrated in Fig. 6. For comparison the results for

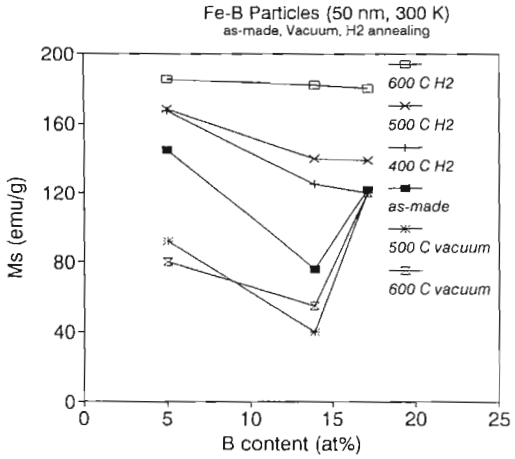

Fig. 6. Saturation magnetization M_s as a function of B content for Fe–B particles (50 nm, 300 K) annealed in vacuum and H_2 at 400, 500 and 600°C. For comparison, the results for the as-made samples are also included.

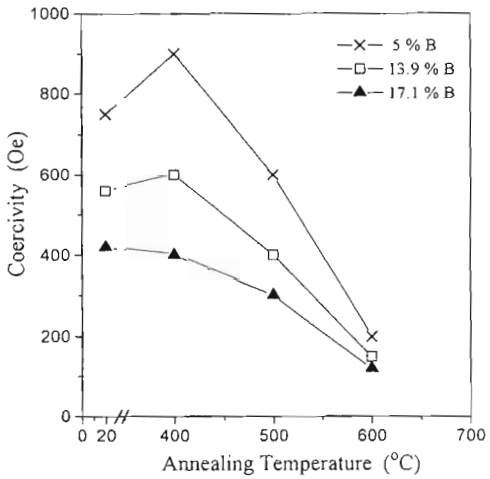

Fig. 7. The coercive field H_c at room temperature as a function of annealing temperature in H_2 for Fe–B particles of three different B concentrations.

the as-made samples are also included in this figure. Annealing in vacuum produces a drastic decrease in magnetization for the low-B-content sample and a decrease to a lesser extent for the medium-B-content sample. The magnetization remains constant for the high-B-content sample. Annealing in H_2 gas at 400°C results in a significant increase of magnetization for the 5% sample and a larger increase for the 14% sample while the magnetization of the 17% samples does not change. When the annealing temperature is raised to 600°C the magnetization shows a strong increase especially for the high-B-content sample to an almost constant value of about 180 emu/g for all three samples.

The effect of annealing in H_2 atmosphere on the coercive field at room temperature is shown in Fig. 7 where H_c is plotted as a function of the annealing temperature for the three different B concentrations. The coercivity, after a slight initial increase at 400°C, decreases monotonously with annealing temperature, the rate of decrease being highest in the low-B-content particles.

Table 1
Mössbauer parameters obtained after analysis of the spectra; δ = isomer shift, ΔEq = quadrupole splitting, H = hyperfine field, ΔH = width of hyperfine field distribution H, % = relative area. Isomer shift values are give relative to α-Fe at RT

Sample	T	δ (mm/s)	ΔEq (mm/s)	H (kG)	ΔH (kG)	%	Phase
5% B, as-made	RT	0.0	0.01	331	3	49	α-Fe
		0.02	0.02	293	4	33	$Fe_{100-x}B_x$
		0.36	0.67	0.0	10	18	Fe–O
	LHe	0.12	0.04	343	3	50	α-Fe
		0.13	−0.02	325	23	27	$Fe_{100-x}B_x$
		0.46	0.04	465	19	14	Fe–O
		0.46	−0.06	509	11	9	Fe–O
14% B, as-made	RT	0.01	0.00	330	1	15	α-Fe
		0.09	−0.05	266	38	50	$Fe_{100-x}B_x$
		0.36	0.72	0.0	20	35	Fe–O
17% B as-made	RT	0.06	−0.02	263	30	45	$Fe_{100-x}B_x$
		0.10	−0.03	220	40	41	$Fe_{100-x}B_x$
		0.036	0.72	0.0	0	14	Fe–O

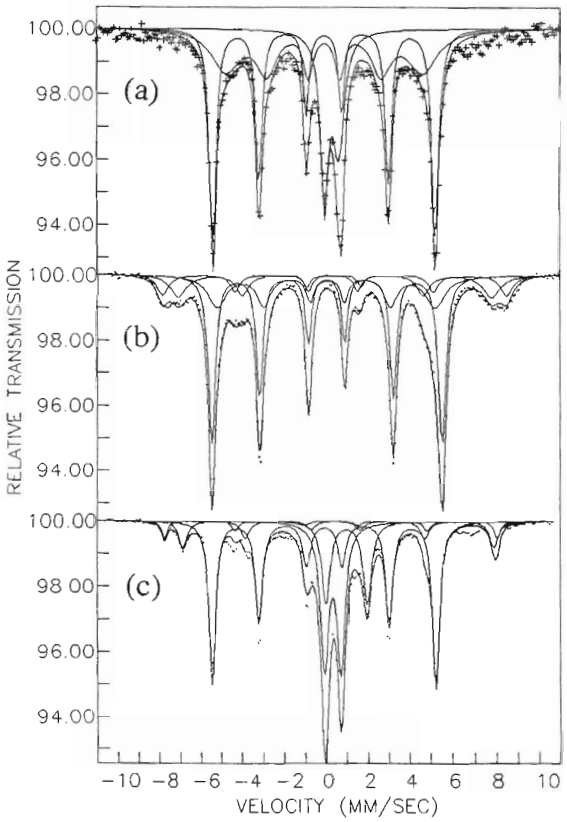

Fig. 8. Mössbauer spectra of Fe–B particles with 5% B: (a) as-made particles at 300 K, (b) as-made particles at 4.2 K, and (c) annealed particles in vacuum at 500°C.

3.3. Mössbauer spectra

The Mössbauer spectra give further information on the phase constitution and magnetic state of the particles studied. A series of Mössbauer spectra for the as-made 5, 14, and 17% samples and samples annealed in vacuum at 500°C for 1 h are shown in Figs. 8–10. Generally, the room temperature spectra are characterized by the presence in various proportions of α-Fe, an amorphous magnetic component with typically broad lines and quadrupole doublets which may be associated with paramagnetic or superparamagnetic phases. The results for the three different concentrations and the effects of annealing are summarized below. A list of the Mössbauer parameters of the various components, and their tentative identification and relative concentrations are given in Tables 1 and 2.

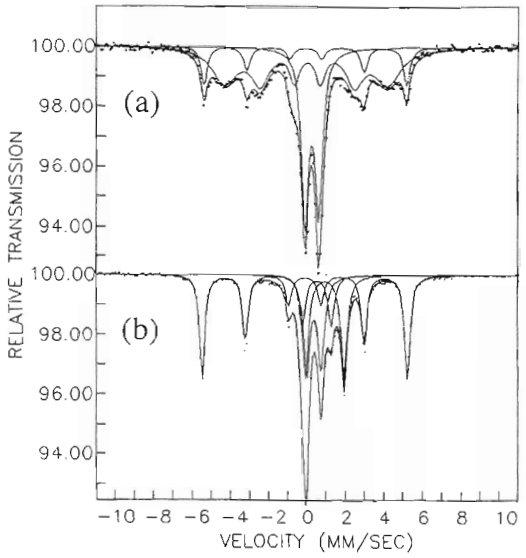

Fig. 9. Room temperature Mössbauer spectra of Fe–B particles with 14% B: (a) as-made, (b) annealed in vacuum at 500°C.

The RT Mössbauer spectrum of the as-made low-B-content (5%) sample is shown in Fig. 8a. It has been analyzed with a superposition of three components: one magnetic sextet with sharp lines attributed to α-Fe, a sextet with broad lines due to an amor-

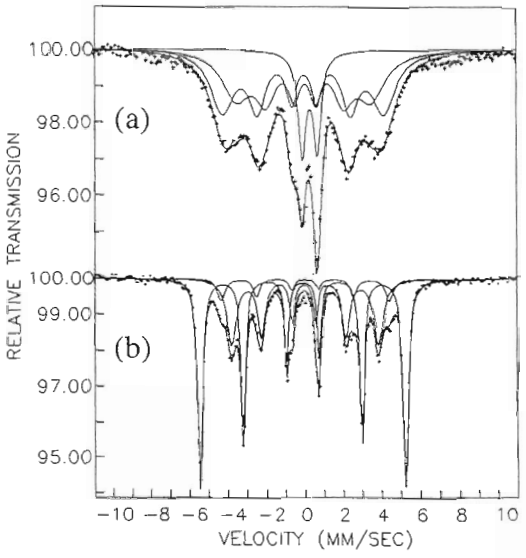

Fig. 10. Room temperature Mössbauer spectra of Fe–B particles with 17% B: (a) as-made, (b) annealed in vacuum at 500°C.

Table 2
Heat-treated samples; Mössbauer parameters obtained after analysis of the spectra; δ = isomer shift, ΔEq = quadrupole splitting, H = hyperfine field, ΔH = width of hyperfine field distribution, % = relative area. Isomer shift values are given relative to α-Fe at RT

Sample	T	δ (mm/s)	ΔEq (mm/s)	H (kG)	ΔH (kG)	%	Phase
5% B, 500°C, vacuum	RT	0.00	−0.01	330	2	47	α-Fe
		0.32	−0.10	492	2	4	Fe_3O_4
		0.60	0.08	460	2	9	
		0.40	0.78	0.0	0	26	Fe^{3+} oct.
		1.06	1.99	0.0	0	15	Fe^{2+} oct.
14% B, 500°C, vacuum	RT	0.00	−0.01	332	1	41	α-Fe
		0.49	0.70	0.0	0	23	Fe^{3+} oct.
		0.65	1.45	0.0	0	12	$Fe^{2.5+}$ oct.
		1.05	2.02	0.0	0	24	Fe^{2+} oct.
17% B, 500°C, vacuum	RT	0.0	0.01	333	2	57	α-Fe
		0.11	0.08	274	7	10	Fe_2B
		0.08	0.08	239	10	33	
5% B, 400°C, H_2	RT	0.00	−0.00	322	30	52	α-Fe
		0.35	0.76	0.0	0	48	Fe–O
14% B, 400°C, H_2	RT	0.01	0.01	323	10	25	α-Fe
		0.08	−0.01	240	36	59	$Fe_{100-x}B_x$
		0.38	0.86	0.0	0	16	Fe–O
17% B, 400°C, H_2	RT	0.00	−0.01	323	40	3	α-Fe
		0.10	−0.02	231	37	87	$Fe_{100-x}B_x$
		0.35	0.80	0.0	0	10	Fe–O
17% B, 500°C, H_2	RT	0.00	0.02	308	10	89	α-Fe
		0.52	0.75	0.0	0	4	Fe^{3+} oct.
		0.99	2.19	0.0	0	7	Fe^{2+} oct.

phous Fe–B component, and a paramagnetic asymmetric doublet attributed to a superparamagnetic Fe oxide. The latter assignment is verified by a measurement at 4.2 K which shows two magnetically split components with broad linewidths and hyperfine parameters, typical of ferric oxides. The nature of this oxide cannot be ascertained but from the room temperature parameters it may be identified as Fe_2O_3. The hyperfine field and the isomer shift values of the amorphous component $Fe_{100-x}B_x$ can give the value of x which is equal to 9 ± 1 according to the calibration charts of Chien et al. [15]. Such high Fe concentration alloys have been reported by Fukamichi et al. [16]. Fig. 8 also shows the room temperature spectrum of the 5% B sample after annealing in vacuum at 500°C for 1 h. Here the presence of a Fe_3O_4 component with large particle sizes is clearly in agreement with the X-ray results. Also, the spectrum shows a prominent α-Fe component as well as two paramagnetic components with parameters consistent with octahedral Fe^{3+} and Fe^{2+}. The former may be due to superparamagnetic Fe_3O_4 (a measurement at 20 K supports this assignment) while the nature of the latter is unclear.

The as-made sample of medium B content (14%) shows a Mössbauer spectrum (Fig. 9a) with a mixture of an amorphous component corresponding to $Fe_{80}B_{20}$ [13] as verified from low temperature Mössbauer data and α-Fe (40 and 25%, respectively). The remaining 35% are related to a paramagnetic doublet with parameters very similar to the component attributed to ferric oxide particles in the low-B-content spectrum as discussed above. Heat treatment in vacuum at 500°C for 1 h leads to the disappearance of the amorphous component due to crystallization, an enhancement of α-Fe and the redistribution of the remaining Fe in three paramagnetic doublets (Fig. 9b) which from the parameters listed in Table 2 may be assigned to Fe^{3+}, $Fe^{2.5+}$, and Fe^{2+}. This result is tentatively consistent with the identification of Fe_3O_4 and Fe_3BO_5 in the X-ray pattern (Fig. 2). Further studies, however, are needed to verify this

assignment since the Mössbauer parameters of Fe_3BO_5 and its magnetic behavior have not yet been studied.

Finally, the room temperature Mössbauer spectrum of the as-made 17% B sample (Fig. 10a) shows magnetic components typical of amorphous Fe–B phases corresponding to average stoichiometry of $Fe_{75}B_{25}$ [13] and a paramagnetic component similar to that observed in the samples with lower boron concentration. Annealing in vacuum at 500°C results in the spectrum of Fig. 10b which is dominated by α-Fe. The remaining iron appears in two magnetically split components with the major component (33%) having hyperfine parameters very close to those of Fe_2B [17]. The other component (10%) has a higher hyperfine field, so it is apparently richer in Fe and it may be assigned to some form of the metastable Fe_3B phase. It should be noted that the X-ray patterns of this sample annealed for 1 h at 500°C do not show the Fe–B phases, apparently because they are in nanocrystalline form. The crystallization of these phases on the other hand has been indicated by the exothermic peak at 475°C in the DSC measurements.

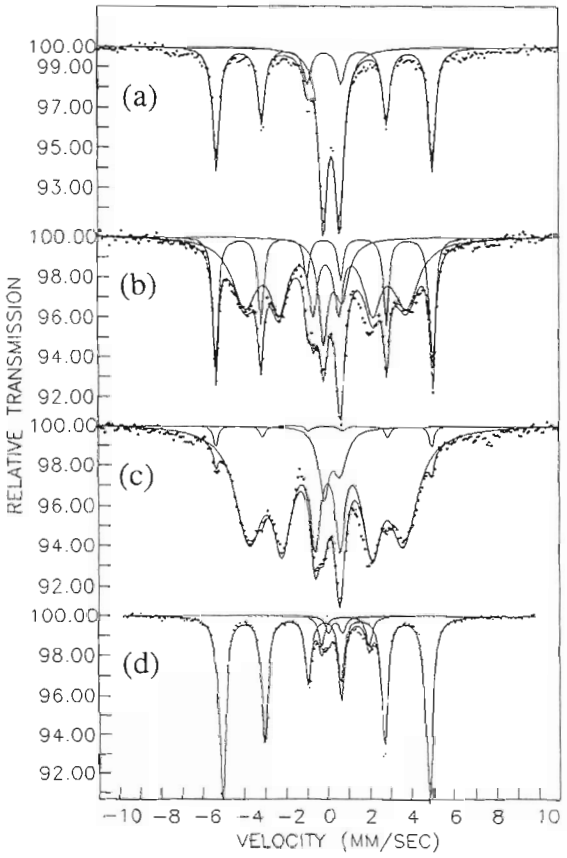

Fig. 11. Room temperature Mössbauer spectra of Fe–B particles annealed in H_2 at 400°C (a) with 5% B, (b) with 14% B, (c) with 17% B, and (d) with 17% B and annealed in H_2 at 500°C.

The Mössbauer spectra of the samples annealed in H_2 gas at 500 to 600°C verify the results from X-ray patterns which show complete crystallization and reduction to α-Fe (Fig. 11). Annealing at 400°C for 1 h results in the reproduction of the original phases (Fig. 11) but with different percentages (Table 2) with the exception of the 5% B sample where the Fe–B amorphous phase is not reproduced. The significant enhancement of the α-Fe component may explain the large increase in magnetization shown in Fig. 6.

4. Discussion

The experimental results obtained on Fe–B fine particles prepared by borohydride reduction, using the different techniques presented in the previous section, can be used to formulate a qualitative model for the processes involved in the formation of the particles and the phase transformations induced in these particles by heat treatment.

In the as-prepared particles a range of B concentrations with 5, 14 and 17 at.% has been obtained, with approximately the same particle size, by keeping the concentration of the reacting solutions constant and varying the rate of addition of the borohydride solution by approximately two orders of magnitude. The composition of the particles consists of α-Fe, an amorphous Fe_xB_{100-x} component, and an oxide component which appears as a paramagnetic doublet in the room temperature Mössbauer spectra. The relative amount of the three components depends on the B content with the highest concentration of amorphous component (85%) observed in the sample with 17% B in agreement with previous studies [13] which indicate that the particles with higher B contents are amorphous. The increase of the amorphous phase with B content is also observed in the X-ray patterns. The oxide component in all samples is superparamagnetic, as demonstrated by low temperature Mössbauer spectra. These data at 85 K

show that only part of the oxide component splits magnetically for the 5 and 17% B-content samples while in the medium-B-content sample the oxide component remains paramagnetic, indicating that the oxide phase exists in a very fine particle size ≤ 10 nm. These oxide components apparently are produced during the drying stage of the preparation due to oxygen impurities in the Ar gas resulting in the passivation of the particles. In accordance with our previous studies of fine iron particles [18] we suggest that the oxide resides on the surface of the particles. We also note that the amount of this component is considerably larger in the medium-B-content particles, in agreement with the minimum magnetization observed in these samples. The phase transformations induced by heat treatment depend strongly on the annealing atmosphere. Annealing at 500°C in vacuum leads generally to crystallization of the amorphous phase as expected from the DSC results which show a crystallization temperature of 475°C. The phases produced by the heat treatment depend on the B content. In the 5% B sample the α-Fe content remains approximately constant (47–49%) and 13% of well crystallized Fe_3O_4 forms which is identified in the X-ray as well as in the Mössbauer spectra. The remaining components are Fe^{2+} and Fe^{3+} phases as witnessed by the Mössbauer parameters. The nature of these phases cannot be ascertained since they are apparently in nanocrystalline state and therefore do not appear in the X-ray patterns. It may be assumed, however, that they are boron containing phases such as Fe_2BO_4, Fe_3BO_5, and/or small particles of $(Fe,B)_3O_4$. The temperature dependence of the Mössbauer spectra could not clarify the particular phase. The hyperfine parameters, corresponding approximately to characteristic values for Fe^{2+} and Fe^{3+} in octahedral coordination with oxygen, are consistent with this assumption.

In the 14% B sample an extended transformation of the iron containing phases occurs as a result of the heat treatment at 500°C in vacuum as shown by the relative concentrations deduced from the analysis of Mössbauer spectra (Table 2). Part of the Fe–B amorphous component crystallizes into α-Fe while the remaining iron and the oxide component are transformed into at least one mixed valence iron phase. This may indicate that the increased B content inhibits oxidation and allows the formation of phases with lower oxidation states. The tentative identification of this component as Fe_3BO_5 or Fe_2BO_4 is consistent with this suggestion. A study of the crystallographic and magnetic structure of these compounds by neutron diffraction has been reported recently [14]. The latter compound shows an onset of antiferromagnetic order between 130 and 160 K while Fe_3BO_5 orders magnetically below 100 K. Mössbauer studies of these mixed valence compounds in bulk form are necessary to identify the phases appearing in the FeB particles since in such a case we can have clear XRD data and the corresponding Mössbauer data.

The 17% boron content particles, which in the as-prepared state show practically only an amorphous component, transform upon heating in vacuum at 500°C predominantly into α-Fe. Boron containing phases, mainly Fe_2B, can be identified only in Mössbauer spectra. They appear in XRD patterns only upon longer annealing or by raising the temperature to 600°C. This observation suggests that the crystallization of the amorphous component proceeds by a separation of α-Fe and Fe–B phases, with the latter initially in nanocrystalline form not observable by XRD.

The heat treatments in H_2 atmosphere above 500°C lead to complete reduction into α-Fe as documented both by XRD and Mössbauer spectroscopy. The question may be raised as to where the boron goes. There is no indication of Fe containing phases in Mössbauer spectra other than α-Fe and the XRD patterns also show essentially only α-Fe. Apparently under H_2 flow gaseous borohydrides are produced which remove B. The magnetization of these particles is close to that of α-Fe. A study of the stability of these particles after passivation would be of interest.

The foregoing discussion leads to a qualitative picture of the role of boron in determining the structure and phase constitution of fine Fe–B particles in the as-prepared state and after various heat treatments. Apart from its effect in promoting amorphous structures in concentrations above $\sim 14\%$, already known from previous investigations, its role as an agent competing with the oxidation of Fe during heat treatment is noteworthy. This is seen most clearly in the medium-B-content particles where mixed valence Fe phases are produced during heat

treatment. Under the conditions of our study, oxygen is apparently introduced into the system during the drying procedure in argon gas, resulting in passivation of the particles, for the low B concentration. At high (17%) B concentrations the formation of an amorphous phase prevents oxidation.

The structural and Mössbauer data can be used to explain the magnetic properties shown in Figs. 5–7. The variation of M_s with B content is believed to be mainly related to the amount of iron oxides present in the samples which is higher in the 14% B sample. The 17% B sample is less oxidized because of its amorphous nature and therefore the magnetization is higher than that of the 14% sample but lower than that of the 5% B sample because of the lower magnetization of the amorphous Fe–B phase compared to the magnetization of Fe. The decrease of coercivity with B content is due to the amount of both the Fe-oxides and the amorphous phase present in the samples (amorphous samples have a lower anisotropy and therefore a lower coercivity). The coercivity decrease and the substantial increase in M_s after annealing in H_2 atmosphere is due to the increased amount of α-Fe because of the reduction of Fe oxides.

5. Conclusion

The results of this work give further insight into the role of preparation parameters and heat treatment for the structural and magnetic properties of Fe–B particles of approximately constant size (~ 50 nm) but with varying B concentration. The annealing data revealed that B acts effectively in preventing oxidation of Fe and that samples with magnetization close to that of α-Fe can be produced by heat treatment in a flow of H_2 gas above 500°C. It would be of interest to study further the stability and passivation properties in these particles.

Acknowledgements

This work was supported in part by NSF DMR 9307676, a NATO collaborative travel grant, and by the PENED program of the Greek GSRD. One of us (GCH) would like to acknowledge the hospitality of the IMS at Demokritos, Athens, and of the Physics Department, University of Ioannina, Greece.

References

[1] H.I. Schlesinger, H.C. Brown, A.E. Finholt, J.R. Galbreath, H.R. Hoekstra and E.K. Hyde, J. Am. Chem. Soc. 75 (1953) 215.
[2] I. Dragieva, G. Gavrolov, D. Buchkov and M. Slavcheva, J. Less-Common Met. 67 (1979) 375.
[3] S.G. Kim and J.R. Brock, J. Colloids Interface Sci. 116 (1987) 431.
[4] A.L. Oppegard, F.J. Darnell and H.C. Miller, J. Appl. Phys. 32 (1961) 184s.
[5] A. Watanabe, T. Uchort, S. Satton and Y. Imaoko, IEEE Trans. Magn. MAG-17 (1981) 1455.
[6] J. van Wonterghem, S. Morup, C.J.W. Koch, S.W. Charles and S. Wells, Nature 332 (1986) 622.
[7] S. Nafis, G.C. Hadjipanayis and C.M. Sorensen, IEEE Trans. Magn. MAG-25 (1989) 3641.
[8] L. Yiping, G.C. Hadjipanayis, C.M. Sorensen and K.J. Klabunde, J. Magn. Magn. Mater. 79 (1989) 321.
[9] L. Yiping, G.C. Hadjipanayis, C.M. Sorensen and K.J. Klabunde, J. Magn. Magn. Mater. 104–107 (1992) 1545.
[10] S. Nafis, G.C. Hadjipanayis, C.M. Sorensen and J.K. Klabunde, J. Appl. Phys. 67 (1990) 4478.
[11] G. Glavee, K.J. Klabunde, C.M. Sorensen and G.C. Hadjipanayis, Langmuir 8 (1992) 771.
[12] S. Linderoth, S. Morup, A. Meagher, J. Larsen, M.D. Bentzon, B.S. Clausen, C.J.W. Koch, S. Wells and S.W. Charles, J. Magn. Magn. Mater. 81 (1989) 138.
[13] S. Wells, S.W. Charles, S. Morup, S. Linderoth, J. van Wonterghem, J. Larsen and M.B. Madsen, J. Phys. Condens. Matter 1 (1989) 8199.
[14] J.P. Attfield, J.F. Clarke and D.A. Perkins, Physica B 180 (1992) 581.
[15] C.L. Chien, D. Musser, E.M. Gyorgy, R.C. Sherwood, H.S. Chen, F.E. Luborsky and J.L. Watter, Phys. Rev. B 20 (1979) 381.
[16] K. Fukamichi, M. Kikuchi, A. Arekawa and T. Masumoto, Solid State Commun. 23 (1977) 955.
[17] I.D. Weisman, L.J. Swartzendruber and L.H. Bennet, Phys. Rev. B 177 (1989) 465.
[18] S. Gangopadhyay, G.C. Hadjipanayis, B. Dale, C.M. Sorensen, K.J. Klabunde, V. Papaefthymiou and A. Kostikas, Phys. Rev. B 45 (1992) 9778.